Optics Letters

Characterizing pump line phase offset of a single-soliton Kerr comb by dual comb interferometry

Ziyun Kong,[1,†,*] Chengying Bao,[1,4,†] Oscar E. Sandoval,[1] Bohao Liu,[1] Cong Wang,[1]
Jose A. Jaramillo-Villegas,[1,2] Minghao Qi,[1,3] and Andrew M. Weiner[1,3]

[1]School of Electrical and Computer Engineering, Purdue University, 465 Northwestern Avenue, West Lafayette, Indiana 47907, USA
[2]Facultad de Ingenierías, Universidad Tecnológica de Pereira, Carrera 27 #10-02, Pereira, Risaralda 660003, Colombia
[3]Birck Nanotechnology Center, Purdue University, 1205 West State Street, West Lafayette, Indiana 47907, USA
[4]Current address: T. J. Watson Laboratory of Applied Physics, California Institute of Technology, Pasadena, California 91125, USA
*Corresponding author: kongz@purdue.edu

We report phase retrieval of a single-soliton Kerr comb using electric field cross-correlation implemented via dual-comb interferometry. The phase profile of the Kerr comb is acquired through the heterodyne beat between the Kerr comb and an electro-optic comb with a pre-characterized phase profile. The soliton Kerr comb has a nearly flat phase profile, and the pump line is observed to show a phase offset which depends on the pumping parameters. The experimental results are in agreement with numerical simulations.   © 2019 Optical Society of America

https://doi.org/10.1364/OL.44.001460

Kerr combs, frequency combs generated by externally pumping high-Q microresonators with a continuous-wave (CW) laser, have seen considerable attention in the last decade [1]. These compact, high-repetition-rate, and potentially complementary metal-oxide-semiconductor compatible comb sources are of interest for a wide range of applications, including optical communications [2], optical arbitrary waveform generation [3], and spectroscopy [4]. Soliton generation, which occurs in anomalous dispersion microresonators, is an important mechanism for the generation of low-noise, broadband Kerr combs with smooth spectra [1,5–8]. In contrast to frequency combs based on mode-locked lasers, the CW pump is coherently coupled to the Kerr comb. An approximate analytic solution for the electric field amplitude of a single-soliton Kerr comb in the framework of the standard Lugiato–Lefever equation (LLE) may be written [5,9]

$$a(t) = a_0 + A e^{i\phi_0} \operatorname{sech}(t/t_p),   \text{(1)}$$

where a_0 is a CW background field, and A, ϕ_0, and t_p are the amplitude, phase shift, and pulse width parameter, respectively, of the soliton. (This field is assumed to repeat every cavity round-trip time.) The complex spectrum consists of a strong line at the pump frequency, superimposed on and phase shifted with respect to the smooth spectral envelope of the soliton. The phase shift of the pump line plays a key role in mediating the parametric gain that affects the comb, and has been shown to be based necessarily

on arguments from a self-organization theory [10]. The existence of such a phase shift has been demonstrated experimentally via a method based on pulse shaping and intensity autocorrelation, both for soliton Kerr combs [8] and dark pulse Kerr combs in normal dispersion microresonators [11].

However, these measurements which rely on optical nonlinearity are difficult and time consuming, especially for soliton Kerr combs that have low power. In this Letter, we demonstrate an all-linear method for phase retrieval of soliton Kerr combs using electric field cross correlation (EFXC) [12], a technique that shares the same technical principle as dual comb spectroscopy [13]. This method delivers rapid waveform measurement and high sensitivity for measurement at low input power. High-quality retrieval of the spectral phase is achieved with 20 μW average power from a 227.5 GHz repetition rate Kerr comb from a planar SiN microring resonator, corresponding to <0.1 fJ per pulse. A similar technique was recently used to capture soliton dynamics in whispering gallery mode microresonators (where the dynamics is slower compared to SiN), but the phase information of the stable solitons was not studied [14,15]. Our experiments confirm that soliton Kerr combs feature a pump line with substantial phase offset with respect to the soliton spectrum which otherwise has nearly flat spectral phase. Moreover, the improved measurement capability now allows us to reveal a significant dependence of the phase offset on pump power and detuning. Numerical simulations based on the LLE [16] show trends similar to those obtained in the experiment.

The experimental setup is illustrated in Fig. 1(a). The system includes two combs (signal comb and reference comb) which differ slightly in repetition rates. Due to the repetition rate difference between the two combs, the reference pulse will sweep across the signal pulse automatically to generate the EFXC signal without any mechanical scan. Equivalently, in the frequency domain, two frequency combs with a slightly different repetition rate heterodyne beat generate a radio-frequency (RF) comb. The phase of the RF comb $\phi_{RF}^i = \phi_{sig}^i - \phi_{ref}^i$ (the superscript i refers to the ith comb line) can be measured by recording the EFXC interferogram. Therefore, the phase of the signal comb (ϕ_{sig}^i) can be obtained once the reference comb
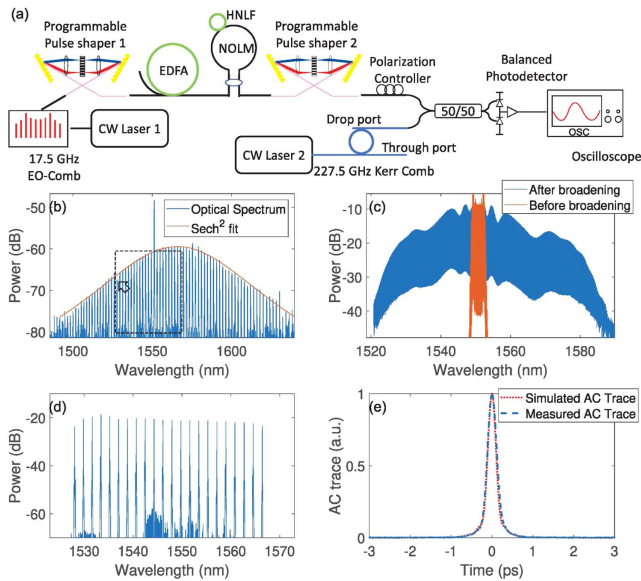
Fig. 1. (a) Experimental setup of the pump phase measurement. Pulse shaper 2 is used to shape the EO comb into a transform-limited pulse with an approximately flat phase profile. CW, continuous-wave; EDFA, erbium-doped fiber amplifier; NOLM, nonlinear optical loop mirror; HNLF, highly nonlinear fiber. (b) Spectrum of the soliton comb; the dashed box indicates the bandwidth covered by our measurements, limited by pulse shaper 2. (c) Spectrum of the EO comb before and after broadening. (d) Spectrum of the broadened EO comb after filtering. (e) Autocorrelation trace of compressed EO comb compared to the simulated trace.

phase (ϕ_{ref}^i) is known. In our experiments, the signal comb is generated from a silicon nitride microresonator (radius 100 μm and loaded-Q 2.4 million) with a repetition rate of ~227.5 GHz [8,17]. We use a drop port which provides a direct sample of the intracavity field. This avoids the complication of a strong superimposed pump field present at the through port [8], which causes a phase shift relative to the intracavity pump field [11]. However, because the drop port has relatively low coupling in order to minimize reduction of the microresonator Q-factor, the output power is reduced. The spectrum of the comb sampled at the drop port, Fig. 1(b), composes a sech²-like spectral envelope together with a ~10 dB stronger pump line corresponding to the weak background accompanying the soliton. Since the repetition rate of the signal comb is high, we use an electro-optic (EO) comb, which also has a relatively high repetition rate, as the reference comb [18]. The spectrum of the generated EO comb is shown as the orange line in Fig. 1(c). A first pulse shaper is used to compress the chirped EO comb into a pulse train. The pulses are then amplified and spectrally broadened within a nonlinear optical loop mirror (NOLM) [19] constructed using highly nonlinear fiber, resulting in spectra that span over 50 nm around at 1550 nm [blue line in Fig. 1(c)]. The NOLM also cleans the pedestal of the associated pulses in the time domain. Since the EO comb is driven by a 17.5 GHz microwave synthesizer (i.e., its repetition rate is 17.5 GHz), only one out of every 13 lines of the EO comb will beat with the soliton Kerr comb to generate low-frequency signals that can be detected by the photodetector. To avoid additive intensity noise associated with the unused EO comb lines, they are filtered out by a

second pulse shaper [see Fig. 1(d) for the filtered EO comb]. The second pulse shaper is also used in a line-by-line pulse-shaping mode [3,11,20] to equalize the intensities of the remaining comb lines and compress them into a transform-limited pulse train at 227.7 GHz, with ~160 MHz repetition rate offset compared to the Kerr comb. When repeated, this procedure returns the same spectral phase within ±0.04 rad (average standard deviation). Figure 1(e) depicts the autocorrelation of the compressed pulses. The close agreement between the measurement and the simulated autocorrelation using the known power spectrum with the assumption of flat spectral phase provides evidence that the compressed pulses are close to transform-limited; hence, we can approximate $\phi_{\mathrm{ref}} \approx 0$.

The input powers (pulse energies) for our dual comb interferometry measurements are typically set at 20 μW (~0.1 fJ) and 1 mW (~5 fJ) for the soliton Kerr comb and the EO comb, respectively. The interferogram is detected by a 20 GHz bandwidth balanced photodetector (Discovery Semiconductor DSC720) and recorded by a Tektronix DSA72004B digital serial analyzer (20 GHz analog bandwidth, 12.5 Gs/s sampling rate). ~7.5 m of Corning SMF-28e fiber connects the microresonator drop-port to the 50/50 fiber coupler; its dispersion is characterized to be 0.135 ps/nm, consistent with the fiber length. Figure 2(a) shows a 20 ns sample of the interferogram. The soliton contributions broaden and blend due to the dispersion and are not clearly visible. However, the Fourier transform of a full 3.2 μs duration interferogram still yields an RF comb, with the power spectrum shown in Fig. 2(c). 23 lines are visible, corresponding to an optical bandwidth of ~5 THz, limited by the passband of pulse shaper 2, used for compression of the broadened reference comb. The line
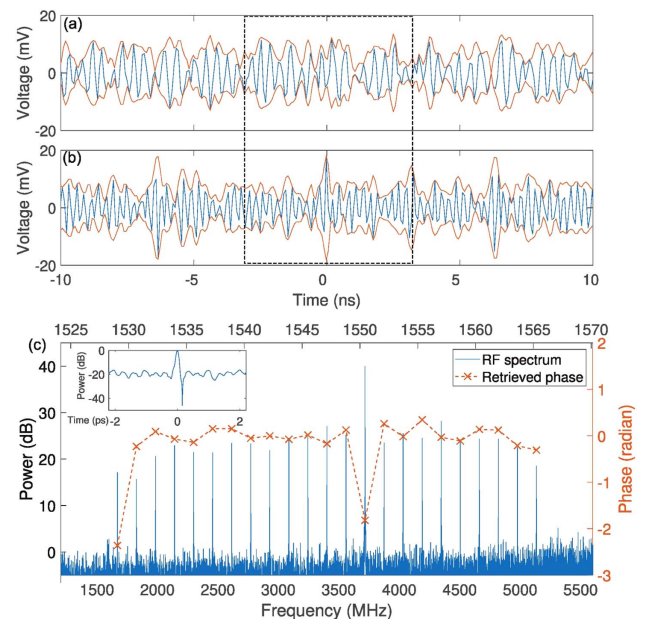

Fig. 2. (a) Portion of the measured time domain interferogram. (b) Reconstructed interferogram after compensating the fiber dispersion, showing isolated RF pulses. The dashed boxes in (a), (b) represent one period of the interferogram, and the orange lines are the envelope of the interferogram. (c) Blue line is the power spectrum of the interferogram. The orange line is the retrieved phase for different optical comb modes, showing a phase offset for the pump line. The inset is the reconstructed intracavity waveform using the measured comb phase.

corresponding to the pump has an SNR exceeding 40 dB; the other lines have SNRs ranging between 17 and 30 dB. Subtracting the phase of the fiber connection and performing an inverse transform yields a corrected interferogram, Fig. 2(b), in which soliton-like peaks begin to emerge. The envelopes of the interferograms, obtained via Hilbert transform, are also plotted. The relatively large background arises due to the truncated spectrum of our reference comb. From the variations of the envelope across different periods, an SNR of ∼4 is estimated for the interferogram in Fig. 2(b), a value consistent with the ratio of the power in the comb lines of Fig. 2(c) to the integrated noise power. The interferogram itself also varies from one period to the next, because its beat and repetition frequencies are not integer multiples. The spectral phase is shown in Fig. 2(c) after correcting for dispersion. The phase of the pump line is shifted by approximately –1.8 rad with respect to the other lines, for which the phase is approximately flat (within ±0.19 rad, roughly one-tenth of the pump phase offset). In the time domain, this corresponds to a soliton with a positive phase shift with respect to the background, consistent with the approximate analytical solution discussed in Refs. [5,9]. Note that the signs of all phases are defined, assuming an $e^{-i\omega t}$ carrier, as in the standard form of the LLE. A phase shift is also observed for the 1528 nm comb line, the shortest wavelength within our measurement range; this may be related to perturbation from the mode interaction [see variations in the spectrum around 1528 nm indicated by the arrow in Fig. 1(b)] [21,22]. Using our phase measurement, we are able to reconstruct the intracavity waveform; see Fig. 2(c). (The comb lines outside the passband of the pulse shaper 2 are assumed to have a zero phase with powers that follow the sech² fit.) There is a dip at the tail of the pulse that is related to the pump phase shift. The origin of this asymmetry will be further addressed in the simulation result below. These results demonstrate that all-linear dual comb interferometry enables characterization of the soliton Kerr comb at low power with high acquisition speed and clearly reveal the phase shift of the soliton with respect to the pump.

The rapid measurement offered by dual comb interferometry allows us to study the dependence of the pump phase offset on pumping conditions. The pump phase offset at a given pumping condition is measured through averaging the retrieved phase of 100 independently captured interferograms. The error bars, taken from the standard deviation among retrieved phase profiles with linear and constant terms removed, are ∼0.08 radian. The measurement results are shown in Fig. 3 for on-chip
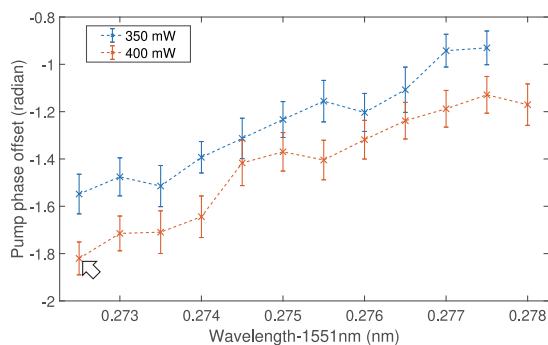

Fig. 3. Retrieved pump line phase offset with increasing pump wavelength (detuning). The point indicated by the arrow corresponds to the data in Fig. 2(c).

pump powers of 350 and 400 mW (estimated based on 3 dB fiber-to-chip coupling loss) for the full range of pump wavelengths over which stable single solitons were obtained. For fixed 400 mW pump power, the phase offset is observed to change from –1.8 rad to –1.2 rad with increasing pump wavelength (corresponding to increasing pump detuning, δ_0, defined below). Moreover, the magnitude of the pump phase offset is larger with increased pump power. From the power spectra and pump phase offsets, we can estimate the behavior in the time domain. The ratio of the soliton peak power to the background is of the order 100 at small detuning and increases by roughly a factor of two as the detuning is increased. The phase of the soliton with respect to the background is positive; the magnitude of the soliton phase offset with respect to the background shows trends similar to Fig. 3 (i.e., the magnitude of the soliton phase offset decreases with increasing detuning). These trends are consistent with the behavior predicted by the approximate analytical solution [5,9].

The measurement results are in reasonable agreement with a numerical simulation based on the generalized LLE with Raman effect included, which can be written as [16,23]

$$\left(\tau_R \frac{\partial}{\partial t} + \frac{\alpha + \theta}{2} + i\delta_0 + i\frac{\beta_2 L}{2}\frac{\partial^2}{\partial\tau^2}\right)E - i(1 - f_R)\gamma L|E|^2 E$$
$$- if_R\gamma L\left(E\int_{-\infty}^{\tau} h_R(\tau - \tau')|E|^2 d\tau'\right) - \sqrt{\theta}E_{in} = 0, \qquad (2)$$

where E is the envelope of the intracavity field; τ_R is the round-trip time (4.4 ps); L is the cavity length (628 μm); τ and t are the fast and slow time, respectively; α and θ are the intrinsic loss and the external coupling coefficient, respectively; β_2 is the group velocity dispersion; γ is the nonlinear coefficient; $|E_{in}|^2$ is the pump power; $\delta_0 = (\omega_o - \omega_p)\tau_R$ is the pump detuning, expressed as a round-trip phase shift (ω_o is the resonance frequency, and ω_p is the pump frequency); and f_R is the Raman fraction. $h_R(\tau)$ is the Raman response function, which is calculated in the frequency domain [23]. The Raman effect is assumed to have a Lorentzian gain spectrum, whose peak is centered at –14.3 THz, and the bandwidth is 2.12 THz. For simplicity, we normalize the pump power and detuning as $X = 8|E_{in}|^2\gamma\theta L/(\alpha + \theta)^3$, $\Delta = 2\delta_0/(\alpha + \theta)$.

For simulations, we choose $\alpha = 0.0024$, $\theta = 0.0011$, $\beta_2 = -61$ ps²/km, $\gamma = 0.9$ W⁻¹ m⁻¹, and $f_R = 0.13$, which we believe are representative of the experimental values. As an example, a stable soliton can be generated by setting the pump power and detuning to $X = 25$ (240 mW) and $\Delta = 13$ (frequency detuning 820 MHz; phase detuning, $\delta_0 = 0.023$). The simulated spectrum of a single soliton, Fig. 4(a), is in good agreement with the measured spectrum. The overall phase profile of the simulated comb is also nearly flat, and there is an offset for the pump line (–2.2 rad). The offset is slightly larger than that in the experiments, which may reflect uncertainties in the experimental parameters used for the simulation. The phase offset of the pump line affects the intracavity time domain waveform, resulting in a dip near the tail of the soliton [Fig. 4(b), similar to the Fig. 2(c) inset]. The waveform is asymmetric (only one dip) as the Raman effect red-shifts the soliton center frequency, resulting in an asymmetric spectrum [24]. If the Raman effect is taken out of the simulation, the waveform is symmetric with dips on both sides. If the Raman is retained, but the pump phase offset is removed, there are no dips on

either side of the soliton. We performed further simulations in which we varied the normalized pump power X and detuning Δ to study how the phase offset of the pump changes with pump parameters. The results are shown in Fig. 4(d) as a function of both X and detuning Δ. In general, we find that the phase offset becomes less negative with increasing pump detuning and decreasing pump power. Figure 4(c) shows two examples of the simulated phase offset versus detuning for fixed pump powers. Furthermore, a comparison between the cases with and without Raman effects shows no significant difference in the pump phase shift. The simulation results are in reasonable agreement with the measurement results in Fig. 3. Qualitatively, we can understand these results if we view the comb line at the pump frequency as arising from the coherent addition of a CW background contribution and a contribution from the soliton spectrum evaluated at the pump frequency. With an increase in detuning, the contribution from the background part decreases relative to that from the soliton. Since the contribution from the soliton at the pump frequency has the same phase as its contributions to other comb lines, the overall phase offset of the pump line with respect to other comb lines tends to decrease as the detuning increases. Note that the self-synchronization theory predicts a negative phase offset between $-\pi/2$ and 0 [10]. Our results also show a negative offset but, in some cases, with magnitude $> \pi/2$. The discrepancy may arise from assumptions in the self-synchronization model; for example, the pump line is assumed to be more than 20 dB stronger than other lines, and other lines have identical powers. Neither of these assumptions holds for the experimental spectrum in Fig. 1(b). Moreover, it was also noted in Ref. [10] that the LLE gives a more negative phase offset than the self-synchronization model.

In conclusion, we have demonstrated phase retrieval of a low power soliton Kerr comb using dual comb interferometry.
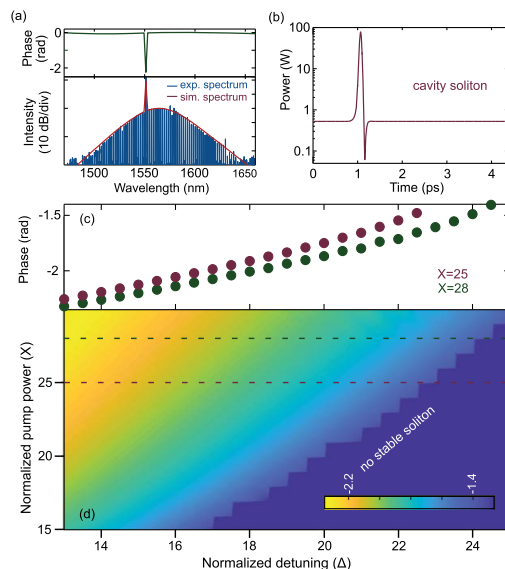
Coupling from the drop port gives us a direct replica of the intracavity pump field and enables the study of the phase for the pump line. With respect to the rest of the spectrum, the pump line is found to have a negative phase offset which becomes more negative with increasing pump power or decreasing pump detuning. This method is especially useful for characterizing signal combs which have very high repetition rates.

REFERENCES

1. T. J. Kippenberg, A. L. Gaeta, M. Lipson, and M. L. Gorodetsky, Science **361**, eaan8083 (2018).
2. P. Marin-Palomo, J. N. Kemal, M. Karpov, A. Kordts, J. Pfeifle, M. H. Pfeiffer, P. Trocha, S. Wolf, V. Brasch, M. H. Anderson, R. Rosenberger, K. Vijayan, W. Freude, T. J. Kippenberg, and C. Koos, Nature **546**, 274 (2017).
3. F. Ferdous, H. Miao, D. E. Leaird, K. Srinivasan, J. Wang, L. Chen, L. T. Varghese, and A. M. Weiner, Nat. Photonics **5**, 770 (2011).
4. M.-G. Suh, Q.-F. Yang, K. Y. Yang, X. Yi, and K. J. Vahala, Science **354**, 600 (2016).
5. T. Herr, V. Brasch, J. D. Jost, C. Y. Wang, N. M. Kondratiev, M. L. Gorodetsky, and T. J. Kippenberg, Nat. Photonics **8**, 145 (2014).
6. X. Yi, Q.-F. Yang, K. Y. Yang, M.-G. Suh, and K. Vahala, Optica **2**, 1078 (2015).
7. C. Joshi, J. K. Jang, K. Luke, X. Ji, S. A. Miller, A. Klenner, Y. Okawachi, M. Lipson, and A. L. Gaeta, Opt. Lett. **41**, 2565 (2016).
8. P.-H. Wang, J. A. Jaramillo-Villegas, Y. Xuan, X. Xue, C. Bao, D. E. Leaird, M. Qi, and A. M. Weiner, Opt. Express **24**, 10890 (2016).
9. S. Wabnitz, Opt. Lett. **18**, 601 (1993).
10. Y. H. Wen, M. R. Lamont, S. H. Strogatz, and A. L. Gaeta, Phys. Rev. A **94**, 063843 (2016).
11. X. Xue, Y. Xuan, Y. Liu, P.-H. Wang, S. Chen, J. Wang, D. E. Leaird, M. Qi, and A. M. Weiner, Nat. Photonics **9**, 594 (2015).
12. F. Ferdous, D. E. Leaird, C.-B. Huang, and A. Weiner, Opt. Lett. **34**, 3875 (2009).
13. I. Coddington, N. Newbury, and W. Swann, Optica **3**, 414 (2016).
14. X. Yi, Q.-F. Yang, K. Y. Yang, and K. Vahala, Nat. Commun. **9**, 3565 (2018).
15. E. Lucas, G. Lihachev, R. Bouchand, N. G. Pavlov, A. S. Raja, M. Karpov, M. L. Gorodetsky, and T. J. Kippenberg, Nat. Photonics **12**, 699 (2018).
16. S. Coen, H. G. Randle, T. Sylvestre, and M. Erkintalo, Opt. Lett. **38**, 37 (2013).
17. C. Bao, Y. Xuan, C. Wang, J. A. Jaramillo-Villegas, D. E. Leaird, M. Qi, and A. M. Weiner, Opt. Lett. **42**, 759 (2017).
18. A. J. Metcalf, V. Torres-Company, D. E. Leaird, and A. M. Weiner, IEEE J. Sel. Top. Quantum Electron. **19**, 231 (2013).
19. V. Ataie, E. Myslivets, B. P.-P. Kuo, N. Alic, and S. Radic, J. Lightwave Technol. **32**, 840 (2014).
20. B. Liu and A. M. Weiner, Opt. Lett. **43**, 4675 (2018).
21. A. B. Matsko, W. Liang, A. A. Savchenkov, D. Eliyahu, and L. Maleki, Opt. Lett. **41**, 2907 (2016).
22. C. Bao, Y. Xuan, D. E. Leaird, S. Wabnitz, M. Qi, and A. M. Weiner, Optica **4**, 1011 (2017).
23. C. Bao, J. A. Jaramillo-Villegas, Y. Xuan, D. E. Leaird, M. Qi, and A. M. Weiner, Phys. Rev. Lett. **117**, 163901 (2016).
24. M. Karpov, H. Guo, A. Kordts, V. Brasch, M. H. Pfeiffer, M. Zervas, M. Geiselmann, and T. J. Kippenberg, Phys. Rev. Lett. **116**, 103902 (2016).

Fig. 4. (a) Example of the simulated spectrum (red) and experimental spectrum (blue) of the soliton Kerr comb with $X = 25$, $\Delta = 13$. The simulated intracavity soliton also has a nearly flat phase profile with the pump line exhibiting a negative phase offset. (b) Intracavity waveform of the simulated cavity soliton. (c) Pump phase offset becomes less negative with increasing detuning for a fixed pump power. (d) Change of the pump phase offset versus pump power and detuning. There is no stable soliton in the dark blue region.